IEEE Access
Multidisciplinary | Rapid Review | Open Access Journal

Received November 8, 2021, accepted November 23, 2021, date of publication November 29, 2021,
date of current version December 7, 2021.

Digital Object Identifier 10.1109/ACCESS.2021.3131211

Backscatter-Aided Relaying for Next-Generation Wireless Communications With SWIPT

AHMAD SIROJUDDIN[1], (Student Member, IEEE), VEZAMAFA NZIMA[1], (Student Member, IEEE), KESHAV SINGH[1], (Member, IEEE), SUDIP BISWAS[2], (Member, IEEE), AND WAN-JEN HUANG[1], (Member, IEEE)

[1]Institute of Communication Engineering, National Sun Yat-sen University, Kaohsiung 80424, Taiwan
[2]Department of Electronics and Communications Engineering, Indian Institute of Information Technology Guwahati, Guwahati, Assam 781015, India

Corresponding author: Keshav Singh (keshav.singh@mail.nsysu.edu.tw)

This work was supported by the Ministry of Science and Technology of Taiwan under Grant MOST 110-2221-E-110-020, Grant MOST 110-2221-E-110-025, and Grant MOST 110-2224-E-110-001. The work of Sudip Biswas was supported by the Science and Engineering Research Board (SERB), DST, Government of India, under Grant SRG/2020/001145. The work of Keshav Singh and Sudip Biswas was supported by the MoU under Grant IIITG/NSYSU 20200728.

ABSTRACT In this paper, we analyze a backscatter network that implements simultaneous wireless information and power transfer. The backscatter devices (BDs) in the network work as relays that receive RF signals from the source, harvest the energy and use it to reflect the signal to the receiver. We assume a non-linear energy harvesting (EH) circuit that takes into account the sensitivity and non-linearity of the electronic components. We formulate an optimization problem to maximize the achievable rate at the receiver of this network. By considering both amplify-and-forward and decode-and-forward modes, we propose algorithms to jointly optimize the power-splitting ratio and the reflection coefficient of the BDs. Simulation results demonstrate the effectiveness of the proposed algorithms with respect to baseline relay networks. In particular, the impact of the number of BDs, source transmit power, and distance of the BDs from the source and destination on the average rate and energy efficiency of the network are illustrated.

INDEX TERMS Backscatter communications system, energy harvesting, relaying scheme, simultaneous wireless information and power transfer.

I. INTRODUCTION

The recent introduction of fifth-generation (5G) standards has brought forward the prospects of massive connectivity in the field of wireless communications and networks [1]. Accordingly, the number of connected devices is expected to increase quite significantly and reach 100 billion by the year 2030 [2]. However, large amounts of transmit power will be required to support the abounding number of devices, which will inevitably lead to high energy costs [3] and increase greenhouse gas emissions [4], [5].

Because of the above, in recent years, energy efficiency has been considered as one of the key metrics due to its commercial and ecological impact [6]. There are several ways in which energy efficiency can be achieved in a wireless communication system, such as efficient resource allocation [7]–[9], optimal network planning [7]–[9], etc. Accordingly, several techniques have been proposed to control the power consumption in wireless communications systems, while also achieving very high capacities. One such technique to improve energy efficiency, while delivering high capacity and better coverage in wireless networks is cooperative communication (CC) [10]. In a cooperative wireless network, messages from the source are relayed to the destination by other devices (users) that act as relay nodes. For example, idle users can use their energy to assist the active users in conveying messages more reliably and effectively. Cooperative networks allow the effective distribution of users to imitate an array of antennas thus achieving spatial diversity gains which include improvements in reliability and capacity. These gains emulate those seen in multiple-input multiple-output (MIMO) systems [11].

A relay is often deployed in either Amplify-and-forward (AF) or decode-and-forward (DF) mode and they can outperform each other depending on the channel conditions from both source to relay and relay to destination, [12].

The associate editor coordinating the review of this manuscript and approving it for publication was Anandakumar Haldorai.

While relays are often seen as coverage extenders, there are instances when they have also been deployed to primarily reduce the transmit power of base stations (BSs) [13]. In particular, besides increasing spectral efficiency, capacity, and coverage, they also offer energy conservation for the BS in that they allow the BS to go into an idle mode more often as users within close proximity communicate with each other without having to route traffic via the network infrastructure [4]. They also enable the users at the edge of the network to receive signals without the BS having to use very high power for transmission since other users can relay the messages from the BS to the edge users [14]. However, since the users utilize their own energy to relay messages, this may lead to decreased battery life and up-time for the users' devices that act as relays. This calls for the use of systems that require very little energy to operate or devices with very high energy efficiencies.

One such technology is backscatter-aided communication that is seen as a promising technique for data transmissions without the need for a conventional energy supply from a battery or power outlet [15]–[22]. In such a system, a backscatter device (BD), which is passive in nature receives an RF signal from an active device, modulates it, and then reflects it to the receiver without having to generate its RF signals. The modulation of the information is performed by varying the reflection coefficient of the antenna. Since the BD does not transmit its RF signals, it consumes orders of magnitude less power than that of other active devices. Hence, such devices can be powered by just harvesting radio frequency (RF) energy from ambient active cellular transmitters. Accordingly, in this paper, we study the concept of a hybrid communication framework that employs backscatter aided relays to perform simultaneous wireless information and power transfer (SWIPT).

A. LITERATURE REVIEW

While several works have shown the utility of wireless backscatter and RF-EH communications (SWIPT in particular) as individual technologies, only a handful of articles have explored them in conjunction with each other. In this sub-section, we first review these two techniques as the basis for self-sustainable RF networks. We then present the works that consider the two technologies in conjunction with each other.

Conventional backscatter communications have been used in many useful applications such as radio-frequency identification (RFID), remote switches, medical telemetry, tracking devices, and low-cost sensor networks to name a few [23], [24]. Nevertheless, several works on backscatter-assisted wireless communication systems have recently been studied [18]–[22]. In [19], the authors proposed a relay cooperation strategy in a backscatter-assisted communication system for IoT to enhance the throughput of the system. Similarly, in [21] a backscatter technology was proposed for wireless communications on high-speed rails which outperforms the direct wireless communication strategy. An iterative algorithm was proposed in [22] for maximizing the energy efficiency for non-orthogonal multiple access (NOMA)-enabled backscatter-assisted communication system.

Next, in cooperative relaying networks, SWIPT has emerged as one of the most promising technologies to extend the lifespan of the network [25]–[29]. In particular, in [25], the outage probability and secrecy outage probability were studied for a SWIPT-enabled full-duplex (FD) jamming system. The authors in [27] proposed user pairing and resource allocation algorithms to maximize the sum rate of a SWIPT-enabled cooperative non-orthogonal multiple access (NOMA) system. Similarly, in [28], the authors considered a dual-hop DF multicasting MIMO relaying system with SWIPT and designed transceivers under both power splitting (PS) based protocol and time switching (TS) based protocols. Further, the SWIPT technology was also investigated for cell-free massive MIMO systems in [28].

Finally, with regards to the two technologies complementing each other, recently, RF-enabled SWIPT has been explored in backscatter-assisted communication system [30]–[35]. In [30], the authors considered a multi-antenna energy transmitter that transmits energy to multiple energy receivers in a backscatter-assisted communication system. The authors then proposed a resource allocation scheme in order to maximize the total utility of the harvested energy by all the receivers. In [31], a backscatter-assisted wireless sensor network with a single hybrid access point and multiple users which operate in both harvest-then-transmit and backscatter modes, was considered. Moreover, an optimal transmission strategy was investigated in [31] to improve the sum-throughput of the network. Next, while the authors in [34] designed a beamforming scheme to maximize the minimum achievable rate in a backscatter-assisted multi-user communication network, a study on the comparison between backscatter communication and RF-EH was presented in [35] for massive IoT networks. Furthermore, in [18], a hybrid harvest-then-transmit backscatter communication mode was proposed for Internet-of-Things (IoT) applications in a wireless powered cognitive radio network. However, to the best of the authors' knowledge, none of the existing works in [30]–[35] have investigated backscatter-assisted relaying schemes with SWIPT. In Table 1, we highlight the differences among conventional relays, backscatter aided communication and the recently evolving intelligent reflecting surface (IRS) aided communication.

The role of a BD can be categorized into two parts: i) the BD can function conventionally by modulating its information with the received RF signal sent from the primary node [36], [37] and then reflect it to the receiver. ii) Alternatively, it may be used purely as a relay in the mold of a conventional cooperative communication method [38], [39], whereby it re-transmits the information received from the source. For the purpose of this study, we consider an ambient backscatter communication system, which acts purely as a relay. We find the best average rate configuration of the

backscattering network and compare it with a conventional relay setup. The primary distinctions of this work are summarized below.

- We consider a backscatter wireless communication system wherein a source sends data to a destination with the aid of multiple BDs. The direct link between source and destination is also taken into account, which is a more general assumption than the one without it.
- The BDs are considered to have wireless energy harvesting capability. Accordingly, the BDs do not need an internal power supply to support their operations. In particular, the BDs receive RF signals from the source, harvests the energy, and use it to reflect the signal to the receiver node. We assume a non-linear energy harvesting circuit that takes into account the sensitivity and non-linearity of components such as inductors, capacitors, and diodes found in the EH circuits. Moreover, the considered model also takes into account the sensitivity power (defined as the minimum power with which the circuit can operate) and the maximum output power.
- We assume that the BDs operate in both AF and DF mode. For each operation, we find the optimal power splitting ratio and the dynamic reflection coefficient to maximize the end-to-end communication achievable rate. We evaluate the system performance (in terms of average rate and energy efficiency) with respect to a baseline system, wherein the BDs are replaced by conventional relays.
- For BDs operating in DF mode, we propose a BD selection scheme to further enhance the end-to-end average rate. The key idea behind this selection is to balance the average rate between the source-to-BDs and BDs-to-destination links.

Paper structure: The paper is structured as follows. Section II describes the system model. The problem formulation for the BD network and corresponding solutions are depicted in Section III and Section IV, respectively. Conventional AF and DF relaying protocols are presented in Section V. Numerical results are provided in Section VI and concluding remarks along with future research directions are provided in Section VII.

II. SYSTEM MODEL

Consider a communication system comprising of a single source (S) which transmits a signal to a destination (D) with the aid of M back-scatter devices (BDs) as shown in Fig. 1. All devices are equipped with a single antenna and all channels experience block Rayleigh fading. Let us define the channels from S to D, S to BDs, and BDs to D as $f \in \mathbb{C}^1$, $\mathbf{h} \in \mathbb{C}^{M\times 1}$, and $\mathbf{g} \in \mathbb{C}^{M\times 1}$, respectively. The corresponding distances from S to D, S to BD, and BD to D are d_f, d_{h_m}, and d_{g_m}, respectively. The signal received by D is expressed as

$$y_d^{(dir)} = \sqrt{P_s} f x + w_d, \tag{1}$$

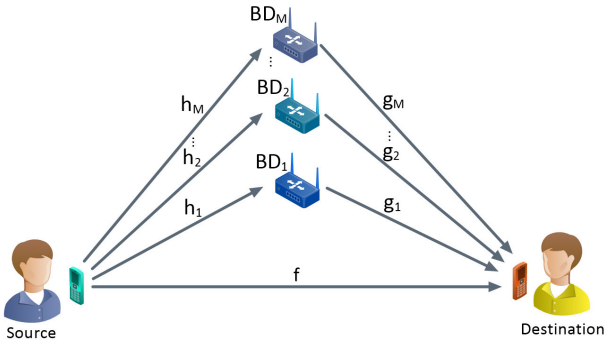

FIGURE 1. An illustration of a BD-assisted relaying network.

where x is the transmitted symbol with $\mathbb{E}\left[|x|^2\right] = 1$ and P_s is the source transmit power. w_d indicates the additive white Gaussian noise (AWGN) with variance σ_d^2. The corresponding SNR can be expressed as

$$\gamma_{s,d}^{dir} = \frac{P_s |f|^2}{\sigma_d^2}. \tag{2}$$

Note that in this work, we consider two modes of operation for the BDs, namely AF and DF, whereby we assume the availability of perfect channel state information (CSI) in both AF and DF communication.

A. BD IN AF MODE (BD-AF)

Here, we consider all the BDs to operate in AF mode i.e., all the BDs simply reflect the received signal from S to the destination D. As a consequence, there is no significant signal processing at the BDs and $S - BD - D$ path of transmission is accomplished within one time slot [40] only. The signal arriving[1] at the m-th BD is expressed as [38]

$$y_m^{AF} = \sqrt{P_s} h_m x, \tag{3}$$

where P_s is the transmit power for the source node S. Inside the m-th BD, the signal is split into two fractions based on the power-splitting coefficient β. The fraction $\sqrt{\beta}$ is absorbed by the BD for its operation and $\sqrt{1-\beta}$ is scattered towards D. The value of $\sqrt{\beta}$ should be adjusted such that it is sufficient to complement the power requirement for the BD's internal circuit operation, P_c. In practice, an RF energy harvesting circuit does not behave linearly. There are various models to find a closed-form relation between the output and input power of such circuits [41], [42]. In this paper, we adopt the model proposed in [42], which is given as

$$P_{out} = \left[\frac{P_{max}}{\exp\left(-\tau P_{sen} + \nu\right)} \left(\frac{1 + \exp(-\tau P_{sen} + \nu)}{1 + \exp(-\tau P_{in} + \nu)} - 1\right)\right]^+. \tag{4}$$

Here, P_{sen} is the energy harvesting circuit sensitivity, P_{max} is the maximum output power of the energy harvesting circuit,

[1] Since the BDs only reflect the signals with particular phase adjustments and do not perform any decoding, interference from the reflected signal to the destination will not affect the incoming signal from the source.

TABLE 1. Differences between the conventional relay, intelligent Reflecting Surface (IRS) and backscatter.

Technology	Operating mechanism	Hardware cost	Energy consumption	Role
Relay / MIMO relay	Active, transmit/receive	High	High	Helper
Intelligent Reflecting Surface (IRS)	Passive reflect	Low	Low	Helper
Backscatter	Passive reflect	Very low	Very low	Source

and ν and τ are parameters obtained from regression for given dataset pairs of P_{in} and P_{out}. The requirement for the BD's operation is that $P_{out} > P_c$. If $P_{in} \triangleq \beta_m P_s |h_m|^2$ is too low, implying that $P_{out} < P_c$ even for $\beta_m = 1$, then the BD's circuit will not have sufficient power to operate and hence it will not be able to backscatter the incoming signal towards D. On the other hand, if $P_{out} = P_c$, then the BD's circuit will work but there will be no power left for backscattering. The reflected signal from the m-th BD is thus expressed as

$$\begin{aligned} x_m^{AF} &= \Gamma_m \sqrt{1-\beta_m} y_m^{AF}, \\ &= \Gamma_m \sqrt{1-\beta_m} \sqrt{P_s} h_m x, \end{aligned} \tag{5}$$

where Γ_m is the complex reflection coefficient of m-th BD and defined as $\Gamma_m = |\Gamma_m| e^{j\theta_m}$. Denote $\mathcal{M} = \{1, \cdots, M\}$, then the subset $\hat{\mathcal{M}} \subseteq \mathcal{M} = \{1, \cdots, M | P_s |h_m|^2 > P_c\}$ is an index set of BDs that can backscatter the signal. The cumulative received signal from the $S-D$ and the $S-BD-D$ links is expressed as

$$y_d^{AF} = y_d^{(dir)} + \sum_{\forall m \in \hat{\mathcal{M}}} g_m x_m^{AF} + w_d, \tag{6}$$

$$= \left(f + \sum_{\forall m \in \hat{\mathcal{M}}} g_m \Gamma_m \sqrt{1-\beta_m} h_m \right) \sqrt{P_s} x + w_d, \tag{7}$$

where w_d is the AWGN at D with zero mean and variance σ_d^2. Then, the end-to-end achievable rate for the system in Fig. 1 with AF backscatter relays is expressed as

$$C_{BD}^{AF} = \log_2 \left(1 + \frac{P_s \left| f + \sum_{\forall m \in \hat{\mathcal{M}}} g_m \Gamma_m \sqrt{1-\beta_m} h_m \right|^2}{\sigma_d^2} \right). \tag{8}$$

B. BD IN DF MODE (BD-DF)

Here, we consider all the BDs to operate in DF mode.[2] Among them, only certain BDs decode the received signal from S in the first time slot. Since BDs do not have a power supply (battery or capacitor to store energy), the operation of all the BDs depend on the RF harvesting power [40]. The incident signal at the m-th BD in the first time slot is expressed as

$$y_m^{DF} = \sqrt{P_s} h_m x + w_{BD,m}, \tag{9}$$

where $w_{BD,m}$ is the AWGN at the m-th BD. The BDs which fail to backscatter the signal due to bad channel conditions are called inactive BDs. Let $\hat{\mathcal{M}}$ denote the set of BDs that successfully decode the signal. Consequently, the SNR for the link between S to the $\hat{m}$-th BD is expressed as

$$\gamma_{s,\hat{m}}^{DF} = \frac{P_s (1-\beta_{\hat{m}}) |h_{\hat{m}}|^2}{\sigma_{\hat{m}}^2}. \tag{10}$$

We redefine and rearrange the elements in $\hat{\mathcal{M}}$ such that $\gamma_{s,1}^{DF} \geq \gamma_{s,2}^{DF} \geq \cdots \geq \gamma_{s,\hat{M}}^{DF}$. Signal decoding is successfully performed by active BDs if the achievable rate is greater than the predefined threshold $R_{\hat{m}}^{(1)}$ as given below

$$C_{\hat{m}}^{(1)} \geq R_{\hat{m}}^{(1)}. \tag{11}$$

Here, $C_{\hat{m}}^{(1)} = \frac{1}{2} \log_2 \left(1 + \gamma_{s,\hat{m}}^{DF}\right)$. Suppose we choose the best $\tilde{M} \leq \hat{M}$ BDs to decode and forward the signal. Then, the rate at the selected BDs is equal to or greater than the rate of the worst performing BD, i.e., $C^{DF,1} \geq C_{\tilde{M}}^{(1)}$. This is to ensure successful decoding of the signal from S by all the active BDs, which is to say that SNR of the first time slot $\gamma_{s,bd}^{DF} \geq \gamma_{s,\tilde{M}}$. In the second time slot, all $\tilde{M}$ selected BDs transmit the signal to D. Thus, the received signal at D can be expressed as

$$y_d^{DF} = \sum_{\tilde{m}=1}^{\tilde{M}} g_{\tilde{m}} \Gamma_{\tilde{m}} \sqrt{1-\beta_{\tilde{m}}} \sqrt{P_s} h_{\tilde{m}} x + w_d, \tag{12}$$

where $g_{\tilde{m}}$ is the channel from the $\hat{m}$th selected BD to D and $\Gamma_{\hat{m}} = |\Gamma_{\hat{m}}| e^{j\theta_{\hat{m}}}$. The received SNR based on (12) is expressed as

$$\gamma_{bd,d}^{DF} = \frac{\left| \sum_{\tilde{m}=1}^{\tilde{M}} g_{\tilde{m}} \Gamma_{\tilde{m}} \sqrt{1-\beta_{\tilde{m}}} \sqrt{P_s} h_{\tilde{m}} \right|^2}{\sigma_d^2}. \tag{13}$$

The end-to-end achievable rate for the system in Fig. 1 with DF backscatter relays is expressed as

$$C^{DF} = \frac{1}{2} \min \left\{ \log_2 \left(1 + \gamma_{s,bd}^{DF}\right), \log_2 \left(1 + \gamma_{s,d}^{DF} + \gamma_{bd,d}^{DF}\right) \right\}. \tag{14}$$

Note: The fraction $1/2$ in (11) and (14) comes from the fact that the transmission requires two time-slots under DF mode.

[2]The BD-DF requires two time-slots since in DF mode, a BD first decodes the incident signal and stores it in a buffer. In the second time-slot, the BD forwards the information to the destination using the unmodulated carrier sent by the source.

III. BD-AF: PROBLEM FORMULATION AND SOLUTION

In this section, we formulate the optimization problem for maximizing the end-to-end achievable rate for the BD-AF scenario.

A. PROBLEM FORMULATION

Using (8), the rate maximization problem for the joint design of power-splitting coefficient β_m and phase shift θ_m under BD-AF scenario is formulated as

$$\begin{aligned}\max_{\{\beta_m,\theta_m\}}\ & \log_2\left(1+\frac{P_s\left|f+\sum\limits_{\forall m\in\hat{\mathcal{M}}} g_m\Gamma_m\sqrt{1-\beta_m}h_m\right|^2}{\sigma_d^2}\right)\\ \text{s.t. }\ & (C.1)\quad P_{out}\left(P_{in}\right)\geq P_c,\\ & (C.2)\quad \theta_m\in[0,2\pi],\quad \forall m\in\hat{\mathcal{M}},\\ & (C.3)\quad 0<\beta_m\leq 1,\quad \forall m\in\hat{\mathcal{M}},\end{aligned}\tag{15}$$

where P_{out} is the harvested power output as a function of P_{in} and is defined in (4). The constraint $(C.1)$ ensures that the output of the energy harvesting circuits of BDs must be enough to run the circuits of BDs, while the constraint $(C.2)$ guarantees that the phase offset of each BD is fully controlled through load modulation [43]. Finally, the constraint $(C.3)$ ensures that the value of the power-splitting coefficient β_m lies between 0 and 1.

Now, the problem of maximizing the achievable rate can be reformulated to maximizing the end-to-end SNR as follows.

$$\begin{aligned}\max_{\{\beta_m,\theta_m\}}\ & \frac{P_s\left|f+\sum\limits_{\forall m\in\hat{\mathcal{M}}} g_m\Gamma_m\sqrt{1-\beta_m}h_m\right|^2}{\sigma_d^2}\\ \text{s.t. }\ & (C.1)\quad P_{out}\left(P_{in}\right)\geq P_c,\\ & (C.2)\quad \theta_m\in[0,2\pi],\quad \forall m\in\hat{\mathcal{M}},\\ & (C.3)\quad 0<\beta_m\leq 1,\quad \forall m\in\hat{\mathcal{M}},\end{aligned}\tag{16}$$

The joint optimization problem (16) is non-convex in the variables β_m and θ_m due to coupling of the variables and thus, it is difficult to solve. Therefore, we adopt an alternating optimization approach where we optimize one variable while keeping the other as a constant.

B. SOLUTION AND PROPOSED ALGORITHM

For a given power-splitting coefficient β_m, the optimization problem (16) can be reformulated as

$$\begin{aligned}\max_{\{\theta_m\}}\ & \frac{P_s\left|f+\sum\limits_{\forall m\in\hat{\mathcal{M}}} g_m\Gamma_m\sqrt{1-\beta_m}h_m\right|^2}{\sigma_d^2}\\ \text{s.t. }\ & (C.2)\quad \theta_m\in[0,2\pi],\quad \forall m\in\hat{\mathcal{M}}.\end{aligned}\tag{17}$$

Since $\Gamma_m = |\Gamma_m|\, e^{j\theta_m}$, we observe that the phase θ_m is a critical design variable for the channel enhancement, while $|\Gamma_m|$ can simply be set to its maximum value in order to increase the reflected signal power [38]. The objective of the problem (17) is to achieve the maximum rate w.r.t. θ_m, if all $\hat{M}+1$ complex scalar terms in the numerator, i.e., f and $g_m\Gamma_m\sqrt{1-\beta_m}h_m, \forall m = 1,\cdots,\hat{M}$ are aligned in the same direction. Note that all the phases can be adjusted except for the first one i.e., f. Accordingly, the values of all θ_m are set such that the term $g_m\Gamma_m\sqrt{1-\beta_m}h_m$ should align in the direction of f. Thus, the optimal θ_m can be obtained as

$$\theta_m^{opt} = \angle\left(fh_m^{\star}g_m^{\star}\right).\tag{18}$$

Now, substituting (18) into the objective function of (17) yields

$$\gamma_{s,d}^{AF} = \frac{P_s\left(|f|+\sum_{m=1}^{\hat{M}}|g_m|\left|\Gamma_m^{\star}\right|\sqrt{1-\beta_m}\,|h_m|\right)^2}{\sigma_d^2}.\tag{19}$$

Using (19) and θ_m^{opt}, the optimization problem (16) can be written as

$$\begin{aligned}\max_{\{\beta_m\}}\ & \frac{P_s\left(|f|+\sum_{m=1}^{\hat{M}}|g_m|\left|\Gamma_m^{\star}\right|\sqrt{1-\beta_m}\,|h_m|\right)^2}{\sigma_d^2}\\ \text{s.t. }\ & (C.1)\quad P_{out}\left(P_{in}\right)\geq P_c,\\ & (C.3)\quad 0<\beta_m\leq 1,\quad \forall m\in\hat{\mathcal{M}}.\end{aligned}\tag{20}$$

It can see that the objective function in (20) monotonically decreases with respect to increasing values of β_m within the range $0<\beta_m<1$. Thus, the optimal β_m^{opt} is set as low as possible while satisfying the harvested energy requirement for the BDs to operate. In other words, $\beta_m^{opt}, \forall m\in\hat{\mathcal{M}}$ are the values that lead to $P_{out}\left(\beta_m\right) = P_c$. Now, rearranging the terms in (4) such that P_{in} is kept in the left-hand-side, we obtain the following expression

$$P_{in}\geq\frac{\nu-\ln\left(\frac{1+\exp(-\tau P_{sen}+\nu)}{1+(P_c/P_{max})\exp(-\tau P_{sen}+\nu)}-1\right)}{\tau}.\tag{21}$$

Since $P_{in} = \beta_m P_s\,|h_m|^2$ and by taking into account that $0<\beta_m\leq 1$, we obtain

$$\beta_m^{opt} = \min\left(\frac{\nu-\ln\left(\frac{1+\exp(-\tau P_{sen}+\nu)}{1+(P_c/P_{max})\exp(-\tau P_{sen}+\nu)}-1\right)}{\tau P_s\,|h_m|^2},1\right).\tag{22}$$

If $\beta_{\hat{m}}^{opt} = 1$, the corresponding term in the numerator of the objective function in (20), i.e. $|g_m|\left|\Gamma_m^{\star}\right|\sqrt{1-\beta_m}\,|h_m|$, is zero, leading to the conclusion that the m-th BD fails to backscatter the incident signal to D. The rate maximization procedure for the BD-AF scenario is summarized in Algorithm 1.

IV. BD-DF: PROBLEM FORMULATION AND SOLUTION

In this section, we formulate the optimization problem for maximizing the achievable rate for the BD-DF scenario.

Algorithm 1 Rate Maximization for BD-AF Scenario

Input: $\mathbf{f}$, $\mathbf{h}$, $\mathbf{g}$, P_S, P_C, P_{sen}, ν, τ.
Output: C^{AF}.
1 Calculate β_m^{opt} by using (22).
2 Obtain $\gamma_{s,d}^{AF}$ using (19) or calculate (18) and then substitute it into the objective of (17).
3 Compute C^{AF} using the objective of (15).

A. PROBLEM FORMULATION

Using (14), the optimization problem for maximizing the achievable rate in the BD-DF network can be formulated as

$$\begin{aligned}\max_{\{\beta_{\tilde{m}},\theta_{\tilde{m}}\},\tilde{M}} \quad & \min\left\{\log_2\left[1+\gamma_{s,bd}^{DF}\right],\log_2\left[1+\gamma_{s,d}^{DF}+\gamma_{bd,d}^{DF}\right]\right\}\\ \text{s.t.} \quad & \left(\overline{C.1}\right) \quad P_{out}\left(P_{in}\right)\geq P_c,\\ & \left(\overline{C.2}\right) \quad \theta_{\tilde{m}}\in[0,2\pi], \quad \forall\tilde{m}\in\hat{\mathcal{M}},\\ & \left(\overline{C.3}\right) \quad 0<\beta_{\tilde{m}}\leq 1, \quad \forall\tilde{m}\in\hat{\mathcal{M}},\\ & \left(\overline{C.4}\right) \quad 0\leq\tilde{M}\leq\hat{M}. \end{aligned} \tag{23}$$

In the above, $\left(\overline{C.1}\right)$-$\left(\overline{C.3}\right)$ are the same as defined for (16), while the constraint $\left(\overline{C.4}\right)$ indicates the number of selected BDs. The formulated problem (23) is non-convex due to the coupling of variables $\beta_{\tilde{m}}$ and $\theta_{\tilde{m}}$, and thus cannot be solved in a straightforward way.

B. SOLUTION AND PROPOSED ALGORITHM

Due to the fact that $\gamma_{bd,d}^{DF}$ is the only term arising due to the reflected signal, it is the only term in the objective function (23) that depends on $\theta_{\tilde{m}}^{opt}$. Now, for given $\tilde{M}$ and $\beta_{\tilde{m}}$, the optimization problem (23) is reformulated to find the optimal $\theta_{\tilde{m}}^{opt}$ as

$$\begin{aligned}\max_{\{\theta_{\tilde{m}}\}} \quad & \gamma_{bd,d}^{DF}=\frac{P_s\left|\sum_{\tilde{m}=1}^{\tilde{M}} g_{\tilde{m}}\Gamma_{\tilde{m}}\sqrt{1-\beta_{\tilde{m}}}h_{\tilde{m}}\right|^2}{\sigma_d^2}\\ \text{s.t.} \quad & \left(\overline{C.3}\right) \quad \theta_{\tilde{m}}\in[0,2\pi], \quad \forall\tilde{m}\in\hat{\mathcal{M}}. \end{aligned} \tag{24}$$

The objective of the problem (24) is to achieve the maximum rate w.r.t. $\theta_{\tilde{m}}$ if all $\tilde{M}$ complex scalar terms in the numerator, i.e., $g_{\tilde{m}}\Gamma_{\tilde{m}}\sqrt{1-\beta_{\tilde{m}}}\sqrt{P_s}h_{\tilde{m}}$, are aligned in the same direction. Since all the terms' phases can be adjusted, the value of $\theta_{\tilde{m}}$ for $\forall m$, is set such that these terms are perfectly aligned to 0^o. Hence, the optimal $\theta_{\tilde{m}}$ is obtained as

$$\theta_{\tilde{m}}^{opt}=\angle\left(h_{\tilde{m}}^{\star}g_{\tilde{m}}^{\star}\right). \tag{25}$$

Substituting (25) into the objective function of the problem (24), the optimal SNR of the link from BD-to-D under the BD-DF case is expressed as

$$\bar{\gamma}_{bd,d}^{DF}=\frac{P_s\left(\sum_{\tilde{m}=1}^{\tilde{M}}|g_{\tilde{m}}|\left|\Gamma_{\tilde{m}}^{\star}\right|\sqrt{1-\beta_{\tilde{m}}}\,|h_{\tilde{m}}|\right)^2}{\sigma_d^2}. \tag{26}$$

For given $\theta_{\tilde{m}}^{opt}$ and $\tilde{M}$, the optimization problem (23) with $\beta_{\tilde{m}}$ as the variable of interest turns into a problem of maximizing (26) with the constraints as expressed in (23) that have correlation with $\beta_{\tilde{m}}$. This can mathematically be given as

$$\begin{aligned}\max_{\{\beta_{\tilde{m}}\}} \quad & \bar{\gamma}_{bd,d}^{DF}\\ \text{s.t.} \quad & \left(\overline{C.1}\right) \quad P_{out}\left(P_{in}\right)\geq P_c,\\ & \left(\overline{C.3}\right) \quad 0<\beta_{\tilde{m}}\leq 1, \quad \forall\tilde{m}\in\hat{\mathcal{M}}. \end{aligned} \tag{27}$$

This problem is similar to (20), where the objective function in (27) is also monotonically decreasing with respect to increasing values of $\beta_{\tilde{m}}$ within the range $0<\beta_{\tilde{m}}<1$. Thus, the solution to (27) with $\beta_{\tilde{m}}$ as the variable of interest is the same as that expressed in (22).

Now, with the optimal $\theta_{\tilde{m}}^{opt}$ and $\beta_{\tilde{m}}^{opt}, \forall\tilde{m}\in\hat{\mathcal{M}}$, the problem (23) with $\tilde{M}$ as the only variable of interest, can be reduced as

$$\begin{aligned}\max_{\tilde{M}} \quad & \min\left\{\log_2\left(1+\gamma_{s,bd}^{DF}\right),\log_2\left(1+\gamma_{s,d}^{DF}+\bar{\gamma}_{bd,d}^{DF}\right)\right\}\\ \text{s.t.} \quad & \left(\overline{C.4}\right) \quad 0\leq\tilde{M}\leq\hat{M}. \end{aligned} \tag{28}$$

Note that $\gamma_{s,bd}^{DF}$ and $\gamma_{bd,d}^{DF}$ in (28) are dependent of $\tilde{M}$ and $\gamma_{s,bd}^{DF}$ is a monotonically decreasing function with respect to the increment in $\hat{M}$ since $\gamma_{s,bd}^{DF}$ is equal to the best $\tilde{M}$ link from S to BD after sorting the channel in a descending order, i.e. $\gamma_{s,bd}^{DF}=\gamma_{s,\tilde{M}}$. Moreover, the best $\gamma_{s,bd}^{DF}$ is obtained when $\tilde{M}=1$, which means that the best link from S to D is chosen. On the contrary, $\gamma_{bd,d}^{DF}$, as expressed in (26), is a monotonically increasing function with respect to the increment in $\hat{M}$ based on the fact that for all non-negative $x_1, x_2, \cdots$, it is true that $\sum_{m=1}^{a}x_m\leq\sum_{m=1}^{b}x_m$ for $a\leq b$. Furthermore, the best $\gamma_{bd,d}^{DF}$ is obtained when $\tilde{M}=\hat{M}$, which means that all the active BDs participate in backscattering the signal towards D.

The rate maximization procedure for the BD-DF scenario is summarized in Algorithm 2, where the optimal $\tilde{M}^{opt}$ is obtained by setting its increment from 1 to the maximum $\hat{M}$. At the beginning, $\gamma_{s,bd}^{DF}$ has the best value and $\gamma_{bd,d}^{DF}$ has the worst value, leading to $C^{DF}(\tilde{M})$ having a low value due to the min operation. As we increment $\tilde{M}$, the value of $\gamma_{s,bd}^{DF}$ decreases and $\gamma_{bd,d}^{DF}$ increases, leading to an improvement in $C^{DF}(\tilde{M})$. At a particular value of $\tilde{M}$, $\gamma_{s,bd}^{DF}<\gamma_{bd,d}^{DF}$, leading to a decrease in $C^{DF}(\tilde{M})$, which is when the iteration is stopped. This particular value of $\tilde{M}$ is set as $\tilde{M}^{opt}$. Additionally, we solve the problems (24) and (27) outside the loop since $\theta_{\tilde{m}}^{opt}$ and $\beta_{\tilde{m}}^{opt}, \forall m\in\hat{\mathcal{M}}$ are independent of $\tilde{M}$. Since the problem (24) and (27) are executed only once, the execution time of Algorithm 2 is quite fast.

V. COMPLEXITY ANALYSIS

For the BDs operating in AF mode, there are two variables to be optimized, namely θ_m and β_m, $\forall m$, where the solution of each is obtained by the closed-form solution (18) and (22), respectively. Since β_m^{opt} does not depend on $\theta_m, \forall m$ and vice versa, the joint optimal solution is obtained by once executing (22) and (18), respectively. Since β_m^{opt} does not depend on

Algorithm 2 Rate Maximization for BD-DF Case

Input: $\mathbf{f}, \mathbf{h}, \mathbf{g}, P_S, P_C, P_{sen}, \nu, \tau$.
Output: C^{DF}.
1 Get $\theta_{\hat{m}}$ and $\beta_{\hat{m}}, \forall \hat{m} \in \hat{\mathcal{M}}$ by solving (24) and (27).
2 Initialize $\tilde{M} = 1, C^{DF(0)} = 0$.
3 **while** $C^{DF(\tilde{M}+1)} > C^{DF(\tilde{M})}$ **do**
4 Increment $\tilde{M}$.
5 Get $C^{DF(\tilde{M})}$ by calculating the objective in (28).
6 **end**

$\theta_m, \forall m$ and vice versa, the joint optimal solution is obtained by once executing (22) followed by (18). In (22), the variable related to each BD is only h_m which appears in the denominator, while the numerator in (22) consists of constants that are independent of m and thus must be computed once. In terms of M, the complexity of (22) is $\mathcal{O}(M)$ since (22) needs to be computed M times. In (18), the number of multiplication and angle operator are fixed and independent of M, but the computation of (18) needs to be repeated $\hat{M}$-times for the active BDs. Hence, the complexity in calculating (18) is $\mathcal{O}\left(\hat{M}\right)$. Thus, the overall complexity[3] of the proposed algorithm for BD-AF network is $\mathcal{O}\left(M + \hat{M}\right)$.

Now, for the BDs operating in DF mode, there are three variables to be optimized, namely $\beta_m, \theta_m, \forall m$, and $\tilde{M}$, where the solution is obtained by (22), (25), and line 3-6 of Alg. 2. Since β_m^{opt} does not depend on $\theta_m, \forall m$ and vice versa, the jointly optimal solution is obtained by once executing (22) followed by (25). As discussed before, the complexity of (22) in terms of M is $\mathcal{O}(M)$. Similar to (18), the number of multiplication and angle operator in (25) are fixed and independent of M, but (25) needs to be executed $\hat{M}$ times for the active BDs. Hence, the complexity of (25) is $\mathcal{O}\left(\hat{M}\right)$. In addition, the BD selection procedure in Algorithm 2 starts with $\tilde{M} = 1$ and is incremented until $C^{DF(\tilde{M}+1)} > C^{DF(\tilde{M})}$. For given $\tilde{M}$, the objective in (28) has complexity $\mathcal{O}\left(\tilde{M}\right)$. Hence, the BD selection procedure has complexity $\mathcal{O}\left(\tilde{M}^2\right)$. Thus, the overall complexity of the proposed BD-DF network becomes $\mathcal{O}\left(M + \hat{M} + \tilde{M}^2\right)$.

VI. NUMERICAL RESULTS

In this section, we analyze the performance of the optimized backscatter network through extensive computer simulations by varying the system parameters.

A. SIMULATION SETUP

Unless otherwise stated, the system parameters are chosen as follows. Each entry of f, h_m, and $g_m, \forall m \in \mathcal{M}$ is the realization of the zero-mean and unit variance complex Normal random variable. The distance between S, D, and BDs are normalized to one. The constants concerning the harvesting energy circuit are set to be $\tau = 274$, $\nu = 0.29$, $P_{max} = 4.927 \times 10^{-3}$ W, $P_{sen} = 6.4 \times 10^{-5}$ W, and $P_c = 8.9 \cdot 10^{-6}$ W [44], [45]. The noise power at BDs and D are -15 dBm. The amplitude of the dynamic reflection coefficient $|\Gamma_m|$ for all BDs is set to 0.7. Any other parameters used will be explicitly mentioned when and wherever used. Next, results from [11], [46] will be used as baseline for comparison of the BD assisted system with conventional relay assisted ones.

[3]Note that the number of active BDs is less than or equal to the total number of BDs in the network, i.e., $\hat{M} \leq M$.

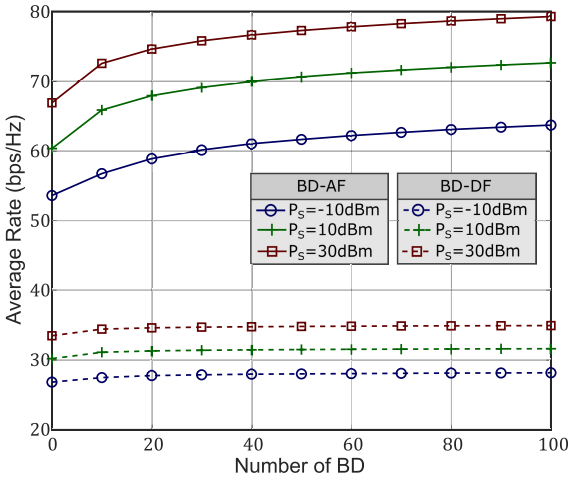

FIGURE 2. Average rate vs. number of BDs with BD operating in AF and DF modes.

B. CSI ACQUISITION

Since the BDs have limited radio resources and signal processing capabilities to send or receive pilot symbols for channel estimation, the source has to estimate all the channels and use them to compute the transmit power allocation as well as the reflection coefficients. The source then provides information on the required reflection configuration (i.e. Γ) to either a micro-controller connected to the BDs or the BDs themselves if they have built-in circuitry. The information can be provided in the form of an index of a pre-defined quantized codebook shared by the source and micro-controller, that contains the various reflection configurations possible at the BDs. Further, techniques such as blind channel estimation [47] and machine learning [48] can also be used to obtain the CSI in such BD-assisted systems.

C. AVERAGE RATE VERSUS NUMBER OF BDs

In Fig. 2, we show the achievable average rate versus the number of BDs in the network. This figure demonstrates that as the number of BDs increases in the network, the achievable rate of the system also increases for both AF and DF cases due to diversity gain. However, the BD-AF case always outperforms the BD-DF case. Further, the average rate increases more rapidly in the region with lower BDs. While the increase in capacity saturates early for the BD-DF case, for the BD-AF case, the growth is consistent with respect to the increasing number of BDs, albeit in a slow manner.

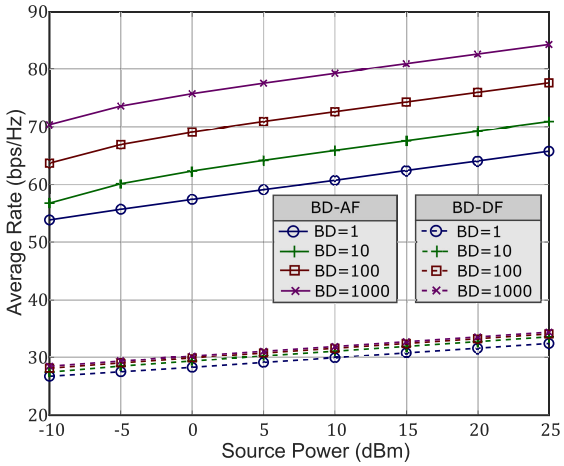

FIGURE 3. Average rate vs. Source power with BD operating in AF and DF.

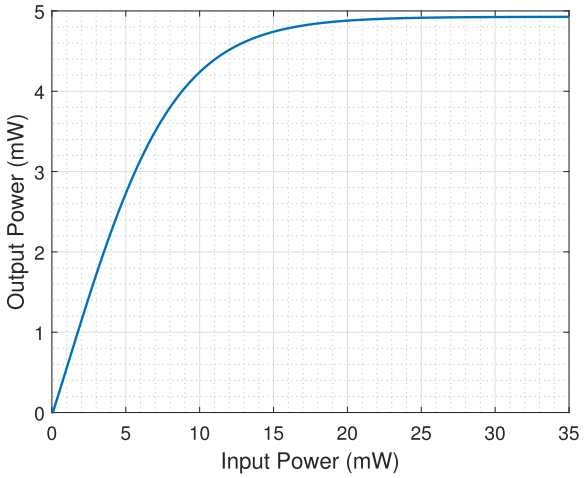

FIGURE 5. P_{out} vs. P_{in} of the non-linear harvesting energy model.

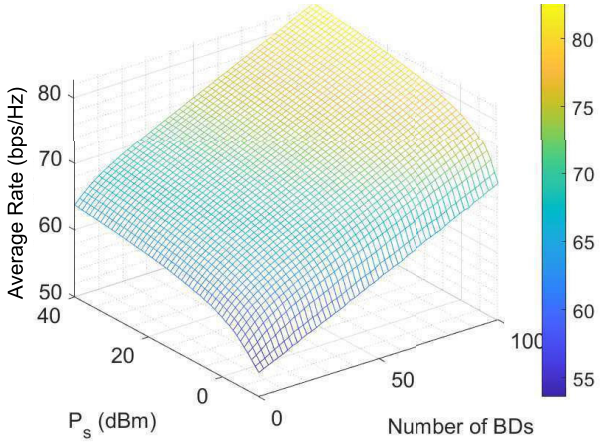

FIGURE 4. Number of active BDs vs. Source power vs. Average rate.

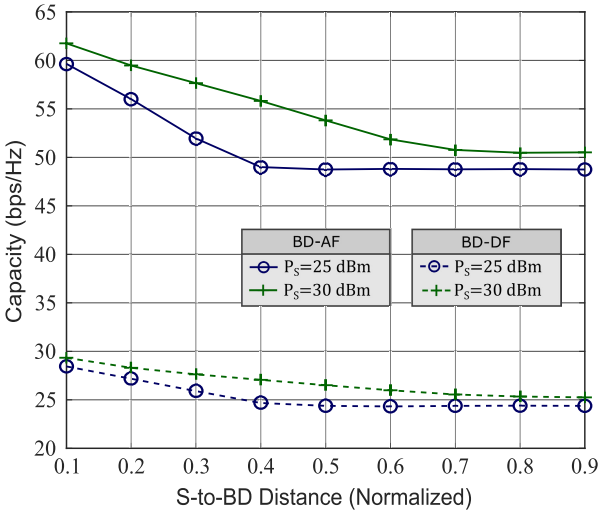

FIGURE 6. Average rate vs. Source to BD distance.

D. AVERAGE RATE VERSUS SOURCE POWER

Fig. 3 shows the average rate versus the transmit power at the source (P_s) for different number of BDs. It can be seen from the figure that the average rate of the system increases as the value of P_s increases. However, the slopes of the curves are somewhat restrained when compared to the increase in transmit power. The increase in average rate with respect to the number of BDs has already been illustrated in Fig. 2 and is further validated here. In particular this figure suggests that average rate of the network can be increased by adding more BDs. In particular this figure suggests that average rate of the network can be increased by adding more BDs, which is an alternative to increasing the transmit power in the network. This result is further validated in 4, which shows that increasing the number of BDs has substantial effect on the average rate of the network as compared to increasing the source transmit power.

E. P_{in} VERSUS P_{out}

Fig. 5 shows the input power P_{in} versus output power P_{out} for the non-linear EH model. The signal power that enters the energy harvesting circuit is not linearly related to the output power of the circuit due to the sensitivity and non-linear performance of components such as diodes, inductors and capacitors [49]. However, from the figure, we can observe that for low values of P_{in}, P_{out} linearly increases with P_{in} before saturating beyond 15 mW.

F. AVERAGE RATE VERSUS SOURCE TO BD DISTANCE

Fig. 6 shows the variation of average rate with respect to the normalized distance between the source and the BD. In particular, the normalized S-BD distance is defined as the S-BD distance divided by the S-D distance. The values 0 and 1 in the x-axis of the figure indicates that the BD is placed at the S and D, respectively. It can be seen from the figure that as the separation between the source and the BDs increase, the performance of the system degrades for both the AF and DF case. The degradation is more significant when the normalized distance is small.

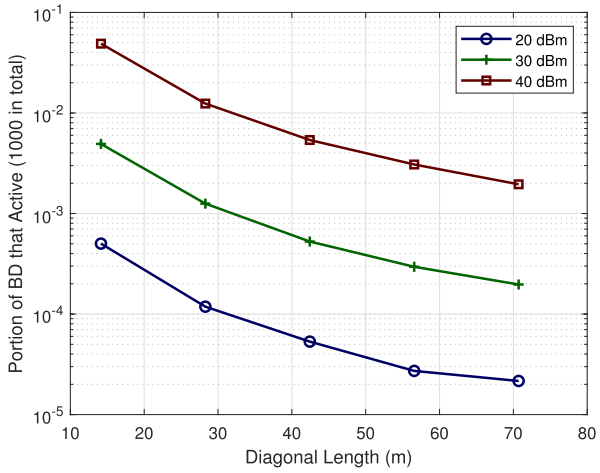

FIGURE 7. Portion of active BDs vs. Diagonal length.

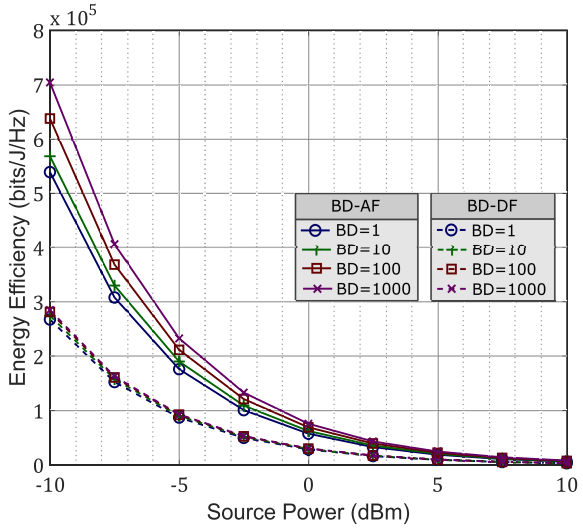

FIGURE 8. Energy efficiency vs. Source power with BD operating in AF and DF.

To understand the effect of the distance on the performance of the system better we formulate an example by considering that the BDs are operating in DF mode only. In particular, within a square area of varying sides, we place 1000 BDs in a uniform but random manner such that they would only be able to decode and forward the signal if they are within a certain distance from the source. We then plot curves using the diagonal of the square for the x-axis and the number of BDs that are active in the y-axis. This is illustrated in Fig. 7, where we can observe that as the size of the square increases, a fewer number of BDs can decode and forward the signal to the destination.

G. ENERGY EFFICIENCY VERSUS SOURCE POWER

Fig. 8 shows the effect of the source transmit power on the EE of the network for varying number of BDs. It can be seen that the EE decreases much faster with the increase in transmit power at the source for BD-AF as compared to BD-DF. However, for the BD-AF case, increasing the number of BDs results in higher efficiency, which indicates that BD aided transmission is indeed energy-efficient. Similar but minuscule effects are also seen for the BD-DF case.

H. COMPARISON OF BD-AF/BD-DF WITH CONVENTIONAL AF/DF RELAY NETWORKS

In this subsection, we compare the average rate performance of the proposed BD-AF and BD-DF networks with respect to baseline AF and DF relay networks. For fair comparison, the total power budget, noise power at the relays and at the destination D are kept the same.

1) AF RELAYING SCHEME

For the system as depicted in Fig. 1 by replacing the BDs with AF relays, the amplifying factor for the m-th relay is given by [11], [46]

$$\alpha_m = \frac{a}{\frac{|g_m|^2\sigma_m^2}{P_S|h_m|^2+\sigma_m^2} + \frac{\sigma_d^2}{P_r}} \frac{\sqrt{P_S}h_m^* g_m^*}{\sqrt{P_S|h_m|^2+\sigma_m^2}}, \tag{29}$$

where P_r is the total transmission power of the relays and a is a constant to satisfy the total relay power constraint. The achievable rate of the system with α_m is given by

$$C^{AF,rel} = \frac{1}{2}\log_2\left(1+\gamma_{s,d}^{dir}+\sum_{m=1}^{M}\frac{\hat{\gamma}_{s,m}\hat{\gamma}_{m,d}}{\hat{\gamma}_{s,m}+\hat{\gamma}_{m,d}+1}\right), \tag{30}$$

where $\hat{\gamma}_{s,m} = P_s|h_m|^2/\sigma_m^2$ and $\hat{\gamma}_{m,d} = P_r|g_m|^2/\sigma_d^2$. Furthermore, the power allocation between S and R can be considered similar [11] to improve the system throughput by introducing a variable ζ such that $0 \leq \zeta \leq 1$. Then, $P_r = \zeta P_{tot}$, $P_S = (1-\zeta)P_{tot}$, and the optimal ζ is obtained as

$$\zeta = \left(\frac{1}{2} - \frac{|f|^2/\sigma_d^2}{\sum_{m=1}^{M}\min\left(\frac{b_m}{1+P_{tot}|h_m|^2/\sigma_m^2}, \frac{b_m}{1+P_{tot}|g_m|^2/\sigma_d^2}\right)}\right)^+, \tag{31}$$

where $b_m = P_{tot}|h_m|^2|g_m|^2/\sigma_m^2\sigma_d^2$.

With the above generalization, we now compare the BD-aided system to a conventional AF relay system with respect to the number of BDs/relays and source transmit power in Fig. 9 and Fig. 10. It can see from the figures that the BD-aided system significantly outperforms the conventional relay based one. For example for equivalent number of BDs/relays, the increase in the average rate of the BD aided system is higher than the relay aided one when the source transmit power increases. Similarly, for fixed source transmit power the increase in the number of BDs produces far better average rate than the relay aided system when equivalent number of relays are increased in the network.

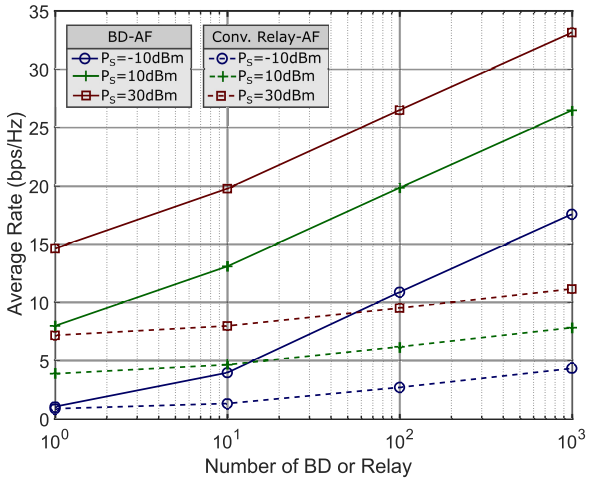

FIGURE 9. Average rate vs. number of AF relays and BDs operate in AF mode.

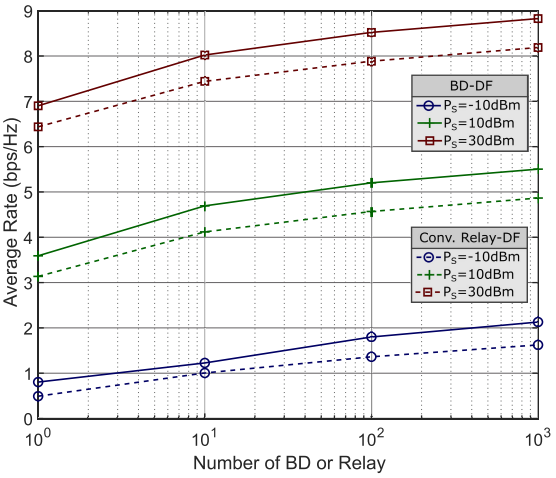

FIGURE 11. Average rate vs. number of BDs for Conventional relay and BD-assisted relay in DF mode.

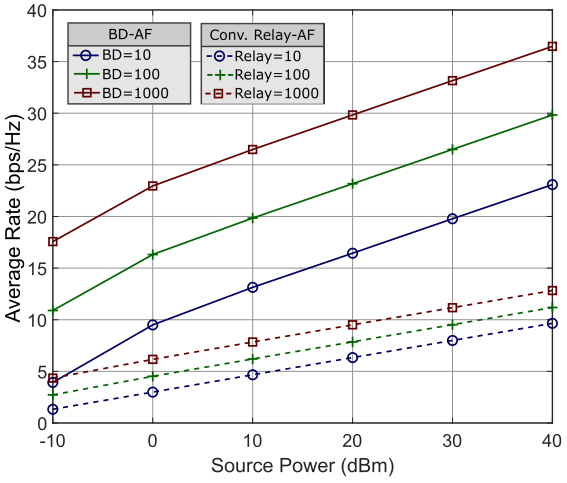

FIGURE 10. Average rate vs. Source Power for Conventional relay and BD-assisted relay in AF mode.

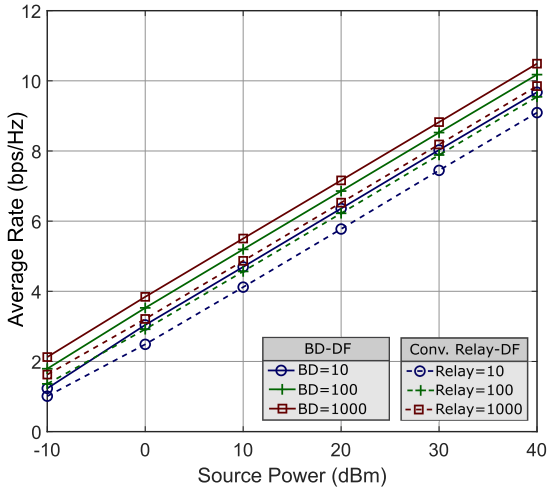

FIGURE 12. Average rate vs. Source Power for Conventional relay and BD-assisted relay in DF mode.

2) DF RELAYING SCHEME

Next, consider a system as depicted in Fig. 1, where the BDs are now replaced by DF relays. Here, in the first time slot, S transmits the signal to both R and D with the rate $R^{DF,1}$. In the second time slot, the set of relays that successfully decode the message, i.e., $\hat{\mathcal{M}} = \{m : \log_2(1+\gamma_{s,m}) \geq 2R\}$ helps in forwarding the source's message to D. It is shown in [11], [50] that the effective SNR at the destination after combining the signal both from the first and second-time slot using maximum ratio combining is given by [50]

$$\gamma_{\text{eff}} = \frac{P_S|f|^2}{\sigma_d^2} + \frac{\sum_{m\in\hat{\mathcal{M}}} P_r|g_m|^2}{\sigma_d^2}. \tag{32}$$

Note that [11] did not consider the design of source transmission rate $R^{DF,1}$, that affects the set of relays $\hat{\mathcal{M}}$ that successfully decode the message with an effective SNR γ_{eff}. Hence, we implement the design of $\hat{\mathcal{M}}$ by incorporating Algorithm 2 into the framework of [11] for a fair comparison. The work in [11] also did not consider the power allocation between S and R. For comparison, we set $P_S = P_r = 0.5P_{tot}$.

The above generalization is now used to compare the BD-aided system to a conventional DF relay system with respect to the number of BDs/relays and source transmit power in Fig. 11 and Fig. 12. Similar to the AF case, the BD-assisted system consistently outperforms the conventional DF-based system. However, unlike the AF case, the gap in performance between the BD and relay-based systems for the DF case is smaller.

VII. CONCLUSION AND FUTURE WORK

We considered a backscatter relay network implementing SWIPT at the BDs. By considering a non-linear EH circuit at the BDs, we formulated an optimization problem to maximize the average rate at the receiver. Both AF and DF modes were considered and algorithms were proposed to jointly optimize the power-splitting ratio and the reflection coefficient of the BDs. Simulation results were performed to assess the impact

of the number of BDs and source transmit power on the performance of the network.

This study provides a reference concerning the use of BDs for achieving high throughput with minimal energy in wireless networks. It can act as a cornerstone to accelerate their implementation in next-generation in future cooperative communications. Nevertheless, certain aspects remain beyond the scope of this paper that may further improve the performance of the system. One such facet is adaptive switching between AF and DF among the BDs, whereby the BDs will always attempt to decode the transmitted data stream from the source. The BDs that can successfully decode the data stream will proceed with the DF operation, while the rest will switch to the AF operation. The above hybrid method will be explored in our future work.

REFERENCES

[1] Q.-U.-U. Nadeem, A. Kammoun, A. Chaaban, M. Debbah, and M.-S. Alouini, "Intelligent reflecting surface assisted wireless communication: Modeling and channel estimation," 2019, *arXiv:1906.02360*.

[2] N. A. Malik and M. Ur-Rehman, "Green communications: Techniques and challenges," *EAI Endorsed Transactions on Energy Web*, vol. 4, no. 14, 2017.

[3] A. Chandra, "Energy conservation in wireless communication systems with relays," in *Proc. Int. Conf. Adv. Mobile Netw., Commun. Appl.*, Aug. 2012, pp. 1–4.

[4] P. Gandotra, R. K. Jha, and S. Jain, "Green communication in next generation cellular networks: A survey," *IEEE Access*, vol. 5, pp. 11727–11758, 2017.

[5] A. Fehske, G. Fettweis, J. Malmodin, and G. Biczok, "The global footprint of mobile communications: The ecological and economic perspective," *IEEE Commun. Mag.*, vol. 49, no. 8, pp. 55–62, Aug. 2011.

[6] R. Q. Hu and Y. Qian, "An energy efficient and spectrum efficient wireless heterogeneous network framework for 5G systems," *IEEE Commun. Mag.*, vol. 52, no. 5, pp. 94–101, May 2014.

[7] F. Meshkati, H. V. Poor, and S. C. Schwartz, "Energy-efficient resource allocation in wireless networks," *IEEE Signal Process. Mag.*, vol. 24, no. 3, pp. 58–68, May 2007.

[8] L. Venturino, A. Zappone, C. Risi, and S. Buzzi, "Energy-efficient scheduling and power allocation in downlink OFDMA networks with base station coordination," *IEEE Trans. Wireless Commun.*, vol. 14, no. 1, pp. 1–14, Jan. 2015.

[9] D. W. K. Ng, E. S. Lo, and R. Schober, "Energy-efficient resource allocation in OFDMA systems with hybrid energy harvesting base station," *IEEE Trans. Wireless Commun.*, vol. 12, no. 7, pp. 3412–3427, Jul. 2013.

[10] M. Amjad, A. Ahmed, M. Naeem, M. Awais, W. Ejaz, and A. Anpalagan, "Resource management in energy harvesting cooperative IoT network under QoS constraints," *Sensors*, vol. 18, no. 10, p. 3560, Oct. 2018.

[11] Y. Hong, W. Huang, and C. Kuo, *Cooperative Communications and Networking: Technologies and System Design*. Springer, 2010.

[12] K. Singh, M.-L. Ku, J.-C. Lin, and T. Ratnarajah, "Toward optimal power control and transfer for energy harvesting amplify- and-forward relay networks," *IEEE Trans. Wireless Commun.*, vol. 17, no. 8, pp. 4971–4986, Aug. 2018.

[13] C. Raman, G. J. Foschini, R. A. Valenzuela, R. D. Yates, and N. B. Mandayam, "Half-duplex relaying in downlink cellular systems," *IEEE Trans. Wireless Commun.*, vol. 10, no. 5, pp. 1396–1404, May 2011.

[14] D. Feng, C. Jiang, G. Lim, L. J. Cimini, Jr., G. Feng, and G. Y. Li, "A survey of energy-efficient wireless communications," *IEEE Commun. Surveys Tuts.*, vol. 15, no. 1, pp. 167–178, 1st Quart., 2013.

[15] G. Vannucci, A. Bletsas, and D. Leigh, "A software-defined radio system for backscatter sensor networks," *IEEE Trans. Wireless Commun.*, vol. 7, no. 6, pp. 2170–2179, Jun. 2008.

[16] A. Bletsas, S. Siachalou, and J. N. Sahalos, "Anti-collision tags for backscatter sensor networks," in *Proc. 38th Eur. Microw. Conf.*, Oct. 2008, pp. 179–182.

[17] J. Kimionis, A. Bletsas, and J. N. Sahalos, "Bistatic backscatter radio for power-limited sensor networks," in *Proc. IEEE Global Commun. Conf. (GLOBECOM)*, Dec. 2013, pp. 353–358.

[18] B. Lyu, H. Guo, Z. Yang, and G. Gui, "Throughput maximization for hybrid backscatter assisted cognitive wireless powered radio networks," *IEEE Internet Things J.*, vol. 5, no. 3, pp. 2015–2024, Jun. 2018.

[19] B. Lyu, Z. Yang, H. Guo, F. Tian, and G. Gui, "Relay cooperation enhanced backscatter communication for Internet-of-Things," *IEEE Internet Things J.*, vol. 6, no. 2, pp. 2860–2871, Apr. 2019.

[20] Y.-C. Liang, Q. Zhang, E. G. Larsson, and G. Y. Li, "Symbiotic radio: Cognitive backscattering communications for future wireless networks," *IEEE Trans. Cognit. Commun. Netw.*, vol. 6, no. 4, pp. 1242–1255, Dec. 2020.

[21] W. Zhao, G. Wang, B. Ai, J. Li, and C. Tellambura, "Backscatter aided wireless communications on high-speed rails: Capacity analysis and transceiver design," *IEEE J. Sel. Areas Commun.*, vol. 38, no. 12, pp. 2864–2874, Dec. 2020.

[22] Y. Xu, Z. Qin, G. Gui, H. Gacanin, H. Sari, and F. Adachi, "Energy efficiency maximization in NOMA enabled backscatter communications with QoS guarantee," *IEEE Wireless Commun. Lett.*, vol. 10, no. 2, pp. 353–357, Feb. 2021.

[23] A. Bletsas, S. Siachalou, and J. N. Sahalos, "Anti-collision backscatter sensor networks," *IEEE Trans. Wireless Commun.*, vol. 8, no. 10, pp. 5018–5029, Oct. 2009.

[24] J. D. Griffin and G. D. Durgin, "Complete link budgets for backscatter-radio and RFID systems," *IEEE Antennas Propag. Mag.*, vol. 51, no. 2, pp. 11–25, Apr. 2009.

[25] R. Ma, H. Wu, J. Ou, S. Yang, and Y. Gao, "Power splitting-based SWIPT systems with full-duplex jamming," *IEEE Trans. Veh. Technol.*, vol. 69, no. 9, pp. 9822–9836, Sep. 2020.

[26] Q. Si, M. Jin, T. A. Tsiftsis, N. Zhao, and X. Wang, "Cooperative SM-based NOMA scheme with SWIPT," *IEEE Trans. Veh. Technol.*, vol. 70, no. 6, pp. 6195–6199, Jun. 2021.

[27] M. Wu, Q. Song, L. Guo, and A. Jamalipour, "Joint user pairing and resource allocation in a SWIPT-enabled cooperative NOMA system," *IEEE Trans. Veh. Technol.*, vol. 70, no. 7, pp. 6826–6840, Jul. 2021.

[28] S. Wang, Z. He, and Y. Rong, "Joint transceiver optimization for DF multicasting MIMO relay systems with wireless information and power transfer," *IEEE Trans. Commun.*, vol. 69, no. 7, pp. 4953–4967, Jul. 2021.

[29] G. Femenias, J. Garcia-Morales, and F. Riera-Palou, "SWIPT-enhanced cell-free massive MIMO networks," *IEEE Trans. Commun.*, vol. 69, no. 8, pp. 5593–5607, Aug. 2021.

[30] G. Yang, C. K. Ho, and Y. L. Guan, "Multi-antenna wireless energy transfer for backscatter communication systems," *IEEE J. Sel. Areas Commun.*, vol. 33, no. 12, pp. 2974–2987, Dec. 2015.

[31] B. Lyu, Z. Yang, G. Gui, and Y. Feng, "Wireless powered communication networks assisted by backscatter communication," *IEEE Access*, vol. 5, pp. 7254–7262, 2017.

[32] Z. B. Zawawi, Y. Huang, and B. Clerckx, "Multiuser wirelessly powered backscatter communications: Nonlinearity, waveform design, and SINR-energy tradeoff," *IEEE Trans. Wireless Commun.*, vol. 18, no. 1, pp. 241–253, Jan. 2019.

[33] F. Rezaei, C. Tellambura, and S. Herath, "Large-scale wireless-powered networks with backscatter communications—A comprehensive survey," *IEEE Open J. Commun. Soc.*, vol. 1, pp. 1100–1130, 2020.

[34] W. Ma, W. Wang, and T. Jiang, "Joint energy harvest and information transfer for energy beamforming in backscatter multiuser networks," *IEEE Trans. Commun.*, vol. 69, no. 2, pp. 1317–1328, Feb. 2021.

[35] R. Du, T. O. Timoudas, and C. Fischione, "Comparing backscatter communication and energy harvesting in massive IoT networks," *IEEE Trans. Wireless Commun.*, early access, Jul. 20, 2021, doi: 10.1109/TWC.2021.3096800.

[36] R. Long, Y.-C. Liang, H. Guo, G. Yang, and R. Zhang, "Symbiotic radio: A new communication paradigm for passive Internet of Things," *IEEE Internet Things J.*, vol. 7, no. 2, pp. 1350–1363, Feb. 2020.

[37] D. Darsena, G. Gelli, and F. Verde, "Modeling and performance analysis of wireless networks with ambient backscatter devices," *IEEE Trans. Commun.*, vol. 65, no. 4, pp. 1797–1814, Jan. 2017.

[38] S. Gong, X. Huang, J. Xu, W. Liu, P. Wang, and D. Niyato, "Backscatter relay communications powered by wireless energy beamforming," *IEEE Trans. Commun.*, vol. 66, no. 7, pp. 3187–3200, Jul. 2018.

[39] S. Gong, Y. Zou, D. T. Hoang, J. Xu, W. Cheng, and D. Niyato, "Capitalizing backscatter-aided hybrid relay communications with wireless energy harvesting," *IEEE Internet Things J.*, vol. 7, no. 9, pp. 8709–8721, Sep. 2020.

[40] X. Jia and X. Zhou, "Performance characterization of relaying using backscatter devices," *IEEE Open J. Commun. Soc.*, vol. 1, pp. 819–834, 2020.
[41] P. N. Alevizos, G. Vougioukas, and A. Bletsas, "Nonlinear energy harvesting models in wireless information and power transfer," in *Proc. IEEE 19th Int. Workshop Signal Process. Adv. Wireless Commun. (SPAWC)*, Jun. 2018, pp. 1–5.
[42] S. Wang, M. Xia, K. Huang, and Y.-C. Wu, "Wirelessly powered two-way communication with nonlinear energy harvesting model: Rate regions under fixed and mobile relay," *IEEE Trans. Wireless Commun.*, vol. 16, no. 12, pp. 8190–8204, Dec. 2017.
[43] S. Gong, J. Xu, D. Niyato, X. Huang, and Z. Han, "Backscatter-aided cooperative relay communications in wireless-powered hybrid radio networks," *IEEE Netw.*, vol. 33, no. 5, pp. 234–241, Sep. 2019.
[44] S. Wang, M. Xia, K. Huang, and Y. Wu, "Wirelessly powered two-way communication with nonlinear energy harvesting model: Rate regions under fixed and mobile relay," *IEEE Trans. Wireless Commun.*, vol. 16, no. 12, pp. 8190–8204, Oct. 2017.
[45] Y. Ye, L. Shi, X. Chu, and G. Lu, "On the outage performance of ambient backscatter communications," *IEEE Internet Things J.*, vol. 7, no. 8, pp. 7265–7278, Aug. 2020.
[46] A. Bletsas, H. Shin, and M. Win, "Outage-optimal cooperative communications with regenerative relays," in *Proc. 40th Annu. Conf. Inf. Sci. Syst.*, Mar. 2006, pp. 632–637.
[47] S. Ma, G. Wang, R. Fan, and C. Tellambura, "Blind channel estimation for ambient backscatter communication systems," *IEEE Commun. Lett.*, vol. 22, no. 6, pp. 1296–1299, Jun. 2018.
[48] S. Ma, Y. Zhu, G. Wang, and R. He, "Machine learning aided channel estimation for ambient backscatter communication systems," in *Proc. IEEE Int. Conf. Commun. Syst. (ICCS)*, Dec. 2018, pp. 67–71.
[49] Y. Lu, K. Xiong, P. Fan, Z. Ding, Z. Zhong, and K. Letaief, "Global energy efficiency in secure MISO SWIPT systems with non-linear power-splitting EH model," *IEEE J. Sel. Areas Commun.*, vol. 37, no. 1, pp. 216–232, Jan. 2019.
[50] P. Kalansuriya and C. Tellambura, "Capacity analysis of a decode-and-forward cooperative network under adaptive transmission," in *Proc. Can. Conf. Electr. Comput. Eng.*, May 2009, pp. 298–303.

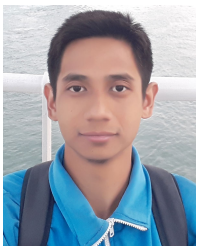

AHMAD SIROJUDDIN (Student Member, IEEE) was born in Malang, Indonesia, in 1994. He received the B.Eng. degree in electrical engineering from Brawijaya University, Malang, Indonesia, in 2016, and the M.S. degree in communications engineering from the National Sun Yat-sen University, Kaohsiung, Taiwan, in 2019, where he is currently pursuing the Ph.D. degree in communications engineering.

His main research interests include signal processing for a two-hop wireless communication system with the assistance of various kinds of devices, such as relay, intelligent reflecting surface, or backscatter devices.

VEZAMAFA NZIMA (Student Member, IEEE) received the B.S. degree in electronics and telecommunication engineering from the University of Eswatini, Kwaluseni, Eswatini, in 2005, and the M.S. degree in telecommunication engineering from National Sun Yat-sen University, Kaohsiung, Taiwan, in 2021.

Since 2009, he has been working with Eswatini Television Authority. He worked as a Maintenance Engineer, a RF Engineer, and is currently the IT Engineer. He was also involved with Eswatini's digital migration from an analogue television system to the current DVB-T2 system the country is currently running. His current research interests include green communications and wireless edge caching.

KESHAV SINGH (Member, IEEE) received the M.Sc. degree in information and telecommunications technologies from Athens Information Technology, Greece, in 2009, and the Ph.D. degree in communication engineering from the National Central University, Taiwan, in 2015. From 2016 to 2019, he was a Research Associate with the Institute of Digital Communications, University of Edinburgh, U.K. From 2019 to 2020, he was associated as a Research Fellow with the University College Dublin, Ireland. He currently works as an Assistant Professor with the Institute of Communications Engineering, National Sun Yat-sen University (NSYSU), Taiwan. His research interests include green communications, resource allocation, full-duplex radio, ultra-reliable low-latency communication, non-orthogonal multiple access, wireless edge caching, machine learning for communications, and large intelligent surface-assisted communications.

SUDIP BISWAS (Member, IEEE) received the Ph.D. degree in digital communications from the University of Edinburgh (UEDIN), U.K., in 2017. He currently works as an Assistant Professor with the Department of Electronics and Communications Engineering, Indian Institute of Information Technology Guwahati (IIITG). He leads research on signal processing for wireless communications, with particular focus on 5G's long-term evolution, including transceiver design for full-duplex radios, wireless edge caching, and comms-radar co-existence and intelligent reflector surface assisted communication. From 2017 to 2019, he was a Research Associate with the Institute of Digital Communications, UEDIN. He also has industrial experience with Tata Consultancy Services, India (Lucknow and Kolkata), where he was an Assistant Systems Engineer, from 2010 to 2012. He was an Organizer of the IEEE International Workshop on Signal Processing Advances in Wireless Communications (SPAWC), Edinburgh, U.K., in 2016, and has been involved in EU FP7 projects: remote radio heads & parasitic antenna arrays (HARP) and dynamic licensed shared access (ADEL), a DST UKIERI project on wireless edge caching and an EPSRC project on NoMA.

WAN-JEN HUANG (Member, IEEE) received the B.S. degree from the Department of Physics, National Taiwan University, Taiwan, in 2001, the M.S. degree from the Institute of Communication Engineering, National Taiwan University, in 2003, and the Ph.D. degree from the Department of Electrical Engineering, University of Southern California, Los Angeles, CA, USA, in 2008. She is currently working as an Associate Professor with the Institute of Communications Engineering, National Sun Yat-sen University, Taiwan. Her research interests include system design and signal processing of cooperative communications and networking, precoding/equalizing for MIMO systems, multiuser detection in CDMA networks, and signal estimation and detection in digital communication systems.